The Wind-driven Circulation in Ocean Basins of Various Shapes

By W. H. MUNK[1] and G. F. CARRIER[2]

(Manuscript received 6 March 1950)

Abstract

The ocean circulation induced by zonal winds has been derived for a triangular ocean basin. The method, which involves the "boundary layer" technique, can be extended to a more general wind system, and to ocean basins of arbitrary shape provided the boundaries are not too irregular. In low and mid-latitudes the principal effect of an inclination, Θ, of the western boundary relative to a north-south direction is to widen the western current (Gulf Stream) by the factor $(\sec \Theta)^{1/3}$ and to reduce the current intensity by a similar factor. A variation in the circulation pattern associated with the variation in the value of the lateral eddy viscosity is noted.

Introduction

The wind-driven circulation in a rectangular ocean basin has been discussed by HIDAKA (1949) and by one of us.[3] The actual shapes of the North Atlantic and North Pacific Oceans deviate greatly from that of a rectangle, but resemble somewhat more closely triangular or semicircular basins, the two cases considered in this paper. The solutions obtained indicate the effect on western currents, such as the Gulf Stream and Kuroshio, of the orientation and curvature of the coast line.

The equation of mass transport and boundary conditions

The stream lines of mass transport, ψ, obey the equation (WOC)

$$\left(A\Delta^4 - \beta \frac{\partial}{\partial x}\right)\psi = -\operatorname{curl}_z \tau, \qquad (1)$$

where A is the kinematic eddy viscosity pertaining to lateral stresses, $\nabla^4 = \partial^4/\partial x^4 + 2\partial^4/\partial x^2 \partial y^2 + \partial^4/\partial y^4$ is the biharmonic operator,

$$\beta = \frac{df}{dy} = \frac{2\Omega}{R}\cos\varphi \qquad (2)$$

is the rate of change northward (positive y) of twice the vertical component of the earth's angular velocity Ω, f the Coriolis parameter, R the earth's radius, φ latitude, and $\operatorname{curl}_z \tau$ the vertical component of the wind stress curl. The positive x-axis extends eastward.

Equation (1) is essentially an integrated version of the vorticity equation, and expresses a balance between three torques: the lateral stress torque, the planetary vorticity, and the wind curl. The equation has been derived (WOC) by integrating the equations of motion (including horizontal and vertical turbulent stresses) from the surface to some depth where the motion and horizontal pressure gradients essentially vanish, and then performing the curl operation. Observations have shown that the velocity of the wind-driven currents at depths of one or two thousand meters equals but a small fraction of the surface velocity.

---

[1] Institute of Geophysics and Scripps Institution of Oceanography, University of California. Contribution from the Scripps Institution of Oceanography, New Series, No. 483. This work has been supported by the Office of Naval Research.

[2] Department of Applied Mathematics, Brown University, Providence, Rhode Island.

[3] W. H. MUNK (1950), *On the Wind-driven Ocean Circulation*, published in the Journal of Meteorology. This article will hereafter be referred to by the symbol (WOC).

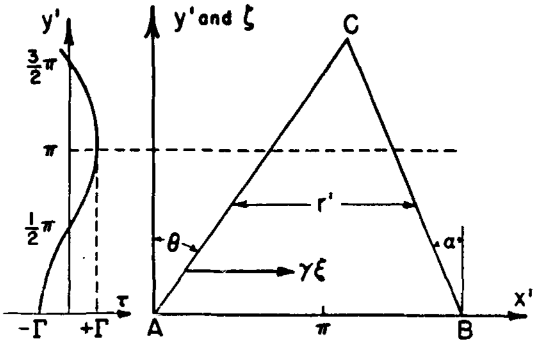

Fig. 1. Dimensions of triangular ocean basin. The wind stress τ varies from $-\Gamma$ at $y' = 0$ ($\varphi = 15°$ N), to $+\Gamma$ at $y' = \pi$ ($\varphi = 50°$ N). A unit distance equals 35° latitude/π, or 1032 km. In these units r' is the latitudinal width of the ocean basin, and $\gamma\xi$ the distance from the western boundary.

Two considerable simplifications result from working with the vertically integrated equations. In the first place, we can examine the case of a baroclinic ocean without having to specify the vertical distribution of density and current; secondly, only the vertical stresses at the upper boundaries need to be specified, and those can be computed from the known wind field over the ocean.

For a wind system we set

$$\tau_x = -\Gamma \cos ny, \quad \tau_y = 0 \tag{3}$$

giving maximum easterlies at $y = 0$ (latitude 15°) and maximum westerlies at $y = \pi/n$ (see fig. 1). The method can easily be extended to an arbitrary distribution of zonal winds, and under certain conditions to a general wind stress field (WOC).

Assume a triangular ocean basin with the dimensions shown in fig. 1. For the boundary conditions along AC and BC we choose

$$\psi_{\text{bdry}} = 0, \quad (\partial\psi/\partial\nu)_{\text{bdry}} = 0 \tag{4a, b}$$

where ν is normal to the boundary. Along AB

$$\psi_{\text{bdry}} = 0, \quad (\partial^2\psi/\partial\nu^2)_{\text{bdry}} = 0. \tag{5a, b}$$

Equations (4a) and (5a) state that the boundary ABCA is a stream line. According to (4b) no slippage takes place along the land boundary ACB, whereas according to (5b) no lateral shear exists along the sea boundary AB. The boundary conditions are equivalent to those imposed on a rigid plate clamped along the coast line ACB and supported along the latitude line AB (WOC).

Solution by boundary layer method

Introducing the non-dimensional parameters $\psi' = \beta\psi/\Gamma$, $r' = nr$, $x' = nx$, $y' = ny$, $n^4\nabla'^4 = \nabla^4$, and writing $k^3 \equiv \beta/A$, equation (1) becomes

$$\left(\gamma^3\nabla'^4 - \frac{\partial}{\partial x'}\right)\psi' = \sin y', \tag{6}$$

where $\gamma = n/k$ is the ratio of the wind wavenumber n to the "Coriolis friction" wavenumber k. The distance π/n between the easterlies and maximum westerlies is roughly 3500 km; it will be shown that

$$\frac{2\pi(\sec\Theta)^{4/3}}{\sqrt{3}\,k}$$

is roughly the latitudinal width of the western currents, say 350 km. Setting $\Theta = 60°$ for the Pacific gives $\gamma \approx .035$.

Inspection of equation (6) now shows that the problem belongs in the "boundary layer" category. The leading term (which contains higher order derivatives than all other terms) has a coefficient $\gamma^3 \ll 1$. The asymptotic solution of equation (6) (i.e., the solution which becomes more and more exact as $\gamma^3 \to 0$) can therefore be anticipated to give a good approximation to the exact flow except in the vicinity of the boundary intersections.

The conventional procedure for obtaining this solution is the following. We find a particular solution of equation (6) by neglecting the term containing γ^3. Such a solution is

$$\psi'^C = -x'\sin y' + d\sin y'. \tag{7}$$

In order to obtain the homogeneous boundary layer solutions which lead to the determination of d and the satisfaction of the boundary conditions, it is convenient to introduce the following coordinate system (fig. 1):

$$\xi = \frac{x'}{\gamma} - \frac{\zeta}{\gamma}\tan\Theta, \quad \zeta = y', \tag{8}$$

so that

$$\psi'^C = (-\gamma\xi - \zeta\tan\Theta + d)\sin\zeta \tag{9}$$

and

$$\frac{\partial}{\partial x'} = \frac{1}{\gamma}\frac{\partial}{\partial \xi}, \frac{\partial}{\partial y'} = -\frac{1}{\gamma}\Phi \tan\Theta \frac{\partial}{\partial \xi} + \frac{\partial}{\partial \zeta}. \tag{10}$$

In equation (10)

$$\Phi(\varphi) = 1 - \frac{\zeta}{\gamma}\frac{d\gamma}{d\zeta} = 1 - \frac{1}{3}(\varphi - \varphi_0)\tan\varphi \tag{11}$$

is a correction involving the *second* derivative of the Coriolis parameter. Here φ_0 is the latitude at which $\gamma = \zeta = 0$, about 15° N. The correction is small at low latitudes and amounts to 25 per cent at 50° latitude.

It is seen that variations in the y-direction involve ζ explicitly as well as implicitly through ξ. Since $\gamma \ll 1$, it follows that only the latter need be considered, so that

$$\nabla'^4 \approx \gamma^{-4} p^{-3}\frac{\partial^4}{\partial \xi^4} \tag{12}$$

where

$$p^{-3} = (1 + \Phi^2 \tan^2\Theta)^2. \tag{13}$$

With these substitutions the asymptotic form of the homogeneous equation becomes

$$\left(\frac{\partial^4}{\partial \xi^4} - p^3\frac{\partial}{\partial \xi}\right)\psi' = 0 \tag{14}$$

with the solution $\psi' = \psi'^W + \psi'^E$, where

$$\psi'^W = \frac{1}{2}(a + ib)\, e^{-\frac{1}{2}(1+\sqrt{3}\,i)p\xi}\sin\zeta + $$
$$+ \frac{1}{2}(a - ib)\, e^{-\frac{1}{2}(1-\sqrt{3}\,i)p\xi}\sin\zeta, \tag{15}$$

$$\psi'^E = c\, e^{-p(r'/\gamma - \xi)}\sin\zeta. \tag{16}$$

It is seen that ψ'^W decreases exponentially with distance from the western boundary and $\psi'^C + \psi'^W$ is therefore the western boundary solution; similiarly $\psi'^C + \psi'^E$ is the eastern boundary solution; whereas ψ'^C is the solution in the central portion of the ocean.

The boundary conditions (5) along AB are already satisfied. The constants a, b, c and d can be evaluated from the boundary conditions along ABCA. Along the western boundary $\xi = 0$, and equations (4 a, b) give

$$-\zeta\tan\Theta + d + a = 0, \quad 2\gamma/p + a - \sqrt{3}\, b = 0.$$

Along the eastern boundary $\xi = r'/\gamma$, where $r' = r_0'(1 - \zeta/\pi)$ is the (non-dimensional) latitudinal width of the ocean, and $r'_0 = (\tan\Theta + \tan\alpha)$ the width at $\zeta = 0$. The eastern boundary conditions give

$$-r' - \zeta\tan\Theta + d + c = 0, \quad -\gamma/p + c = 0.$$

The boundary conditions can be combined to yield

$$a = -r'(1 - \varepsilon), \quad c = r'\varepsilon,$$
$$\sqrt{3}\, b = -r'(1 - 3\varepsilon), \quad d = r'(1 - \varepsilon) + \zeta\tan\Theta, \tag{17}$$

where $\varepsilon = \gamma/pr'$ is a small quantity. The approximation involved in the non-homogeneous term (7) can now be estimated by performing the operation indicated in equation (6) on ψ'^C:

$$\left(\gamma^3 \Delta'^4 - \frac{\partial}{\partial x'}\right)\psi'^C = \sin y'\,[1 - \gamma^3(d - x')].$$

The exact solution requires that the right side equal $\sin y'$. Since $d - x' = r'(1 - \varepsilon) - \gamma\xi$, or r' at most, the neglected term is less than $\gamma^3 r'$, that is less than 1 per cent.

The solution becomes

$$\psi' = r'\sin\zeta\Bigg[-\frac{2}{\sqrt{3}}\left(1 - \frac{3}{2}\varepsilon\right)e^{-\frac{1}{2}p\xi}\cos\left(\frac{\sqrt{3}}{2}p\xi + \frac{\sqrt{3}}{2}\varepsilon - \frac{\pi}{6}\right) + 1 - $$
$$-\varepsilon\left(p\xi - e^{p\xi - 1/\varepsilon} - 1\right)\Bigg]. \tag{18}$$

For north-south boundaries, $\Theta = 0$, $p = 1$, and the equation reduces to the rectangular case discussed in (WOC). The first term in the bracket gives the variation of ψ' with x near the western boundary, as shown in fig. 2. It indicates a series of exponentially "damped" boundary vortices, with a strong north-flowing current and countercurrent in the western vortex, both of latitudinal width $2\pi/\sqrt{3}$ pk. The principal effect of the inclined western coast line is to widen the western current (measured normal to the boundary) by the factor

$$p^{-1}\cos\Theta \approx (\sec\Theta)^{1/3}$$

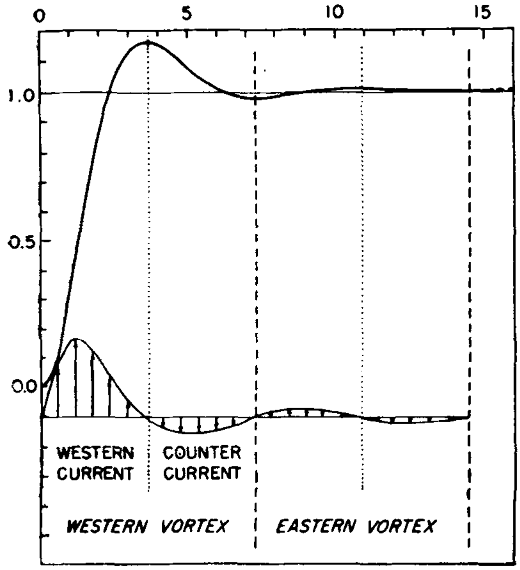

Fig. 2. East-west variation of ψ' near the western boundary for an infinitely wide ocean [equation (18) with $\varepsilon = 0$]. The arrows indicate the direction and intensity of the long-shore component of the current. Compare with Figures 4 to 6.

and to reduce the current intensity by a similar factor. The approximation refers to low latitudes; in high latitudes the modification associated with an inclination of the coast line is reduced, or even reversed. The total transport remains approximately the same. The inclination of the eastern boundary is important only insofar as it involves the width r of the oceans.

Circulation of the Pacific Ocean

Fig. 3 shows a chart of the Pacific Ocean on which north-south and west-east distances have been preserved. The basin north of 15° N is approximated by an isosceles triangle with a base of 13 units and altitude of 4 units (1 unit = 1032 km, see fig. 1). A rectangle is also drawn, which has the proper width at a latitude of 32.5° N midway between the easterly and westerly winds.

Figs. 4—6 show the computed stream lines in the triangular and rectangular ocean basins for the following numerical values of the parameters:

	Fig. 4	Fig. 5	Fig. 6
Shape of basin	triangle	rectangle	triangle
A in $cm^2\,sec^{-1}$	$2.5 \cdot 10^7$	$2.5 \cdot 10^7$	10^8
π/n	35° lat.	35° lat.	35° lat.
At 30° N latitude:			
k in cm^{-1}	$2.0 \cdot 10^{-7}$	$2.0 \cdot 10^{-7}$	$1.25 \cdot 10^{-7}$
γ	.040	0.040	.064
p	.445	1.00	.445
$\dfrac{2\pi}{\sqrt{3pk}}$ in km	410	182	650
$\dfrac{2\pi}{\sqrt{3pk}} \cos\Theta$ in km	215	182	341

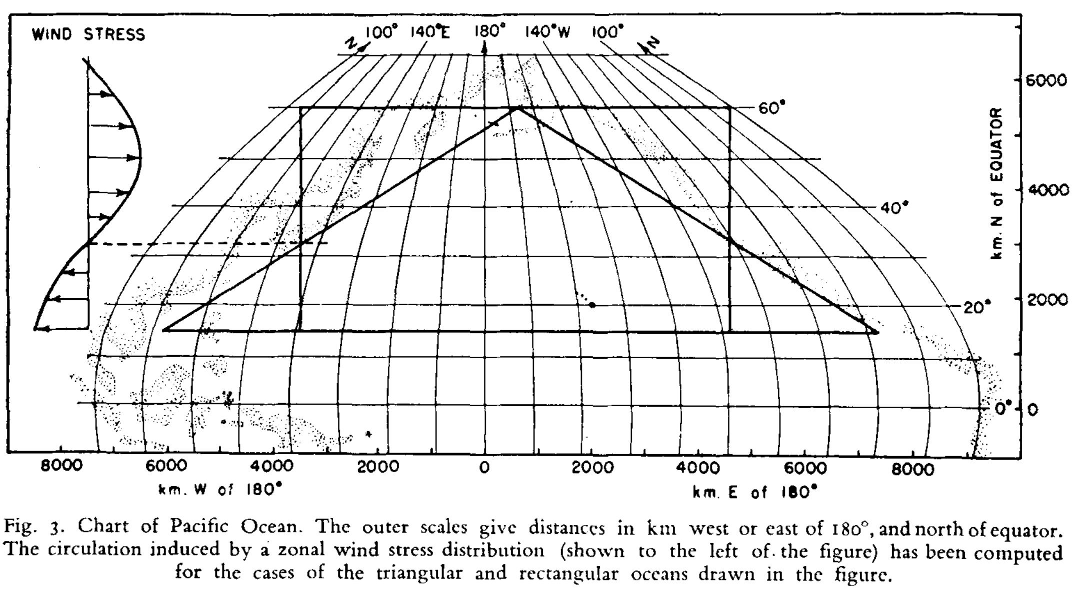

Fig. 3. Chart of Pacific Ocean. The outer scales give distances in km west or east of 180°, and north of equator. The circulation induced by a zonal wind stress distribution (shown to the left of the figure) has been computed for the cases of the triangular and rectangular oceans drawn in the figure.

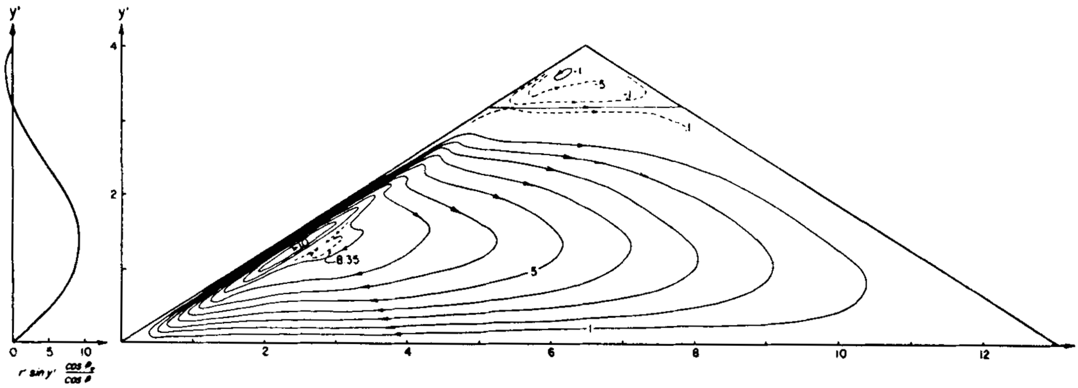

Fig. 4. Computed transport stream lines in the triangular ocean basin for $A = 2.5 \cdot 10^7$ cm² sec⁻¹. The lines represent equal values of $(\beta_0/\Gamma)\psi$. The curve to the left represents the variation of ψ with latitude. Unit distances along the x- and y-axis equal 1032 km. The section between $x = 1.5$ and $x = 4.0$, $y = 0.5$ and $y = 2.0$ has been redrawn on an enlarged scale in Figure 8.

The last two lines give the latitudinal and actual widths of the western current and countercurrent at the latitude 30°N where these currents attain their maximum intensity.

The stream lines are drawn[1] for equal values of

$$\frac{\beta_0}{\Gamma}\psi = \frac{\cos\varphi_0}{\cos\varphi}\, r' \sin\zeta\, [f(p\xi, \varepsilon)] \qquad (19)$$

where β_0 is the value of β at y' = 0. The function in the bracket is the one in equation (18). The expression preceding the bracket is a function of y only, and shown to the left of figs 4 and 5. In the case of the triangular ocean this function vanishes at latitudes 15° N, 50° N and 60° N, and accordingly divides the circulation into an anticyclonic and a cyclonic gyre. These gyres have been named the subtropical and subpolar gyres (WOC), and correspond roughly to the regions of the subtropical anticyclones and of the cyclonic storms, respectively. In the case of the rec-

[1] The approximations involved break down near the northern vertex of the triangle where the 2 boundary strips overlap. In this region the stream lines have been estimated. Because the real and abstracted boundaries differ greatly in this small region, it seems hardly worthwhile to devise special methods to compute the exact position of the theoretical stream lines.

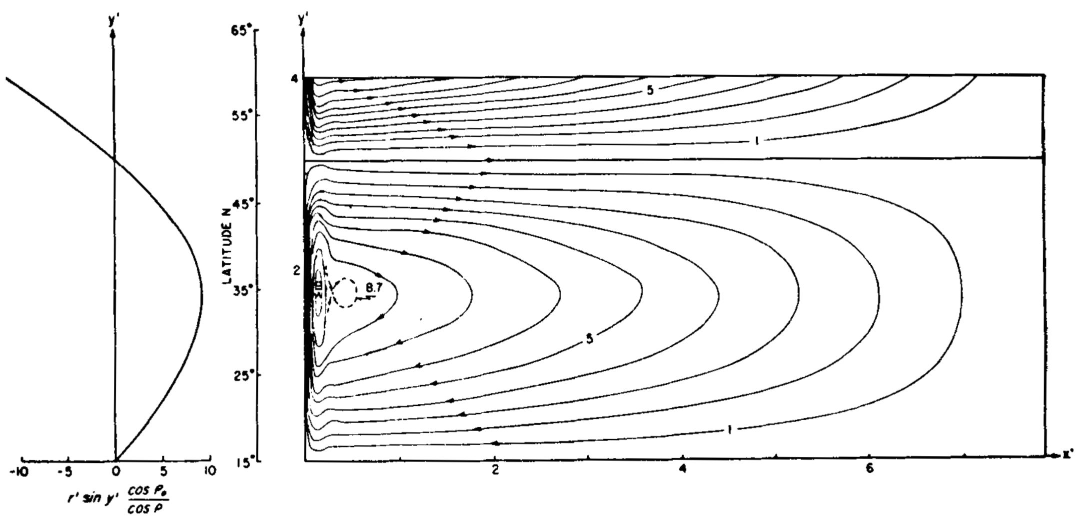

Fig. 5. Computed transport streamlines in the rectangular ocean basin for $A = 2.5 \cdot 10^7$ cm² sec⁻¹.

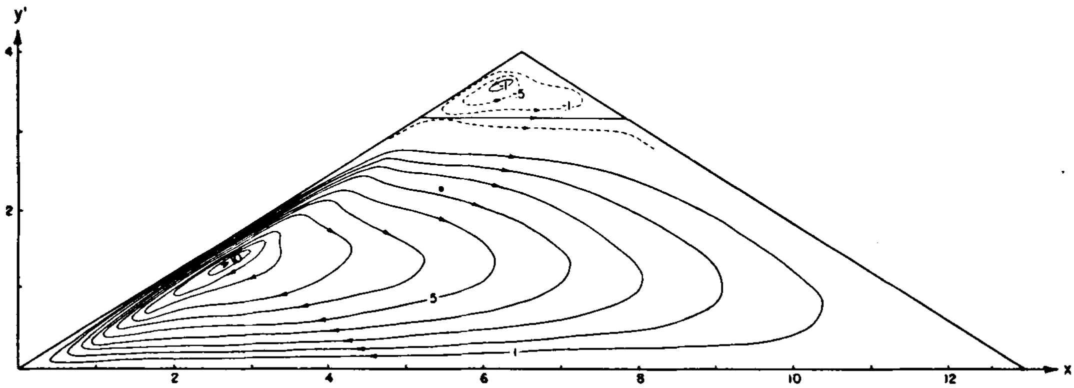

Fig. 6. Computed transport stream lines in the triangular ocean basin for $A = 10^8$ cm^2 sec^{-1}.

tangular ocean only part of the subpolar gyre is included.

The location and intensity of the gyres on figs. 4 and 6 compares favorably with oceanographic measurements, as presented in fig. 7. Note that the maximum transport of the western (Kuroshio) current takes place at 30° N latitude; that the ratio of mass transport of the Kuroshio Current to that of the Oyashio Current is of the order of 10:1. The eastern Pacific gyre and the California Current are the result of local meridional winds (WOC) and are therefore not present in our model for zonal winds.

Discrepancy between observed and computed transport

Computations based on the available wind data and the best available information concerning the relationship between wind speed at anemometer level and the stress exerted on the sea surface gives $\Gamma = 0.65$ dynes cm^{-2}. (WOC) Setting $\beta_0 = 2.2 \cdot 10^{-13}$ cm^{-1} sec^{-1} one finds that each unit of $\beta_0\,\psi/\Gamma$ as drawn on figs. 4—6 represents a transport of $3 \cdot 10^{12}$ *g* sec^{-1}, or 3 million metric tons sec^{-1}. This is one half the contour interval in fig. 7. We conclude that the computed *pattern* of water transport resembles the observed pattern quite closely, whereas the computed *quantity* of transport is about half the observed quantity.

This discrepancy cannot be ascribed to the value of the eddy viscosity, for, according to equation (18), the transport is almost independent of A. Nor can the discrepancy be ascribed to our assumption of no slippage against the western boundary. Taking the extreme case of *free slippage* against the western

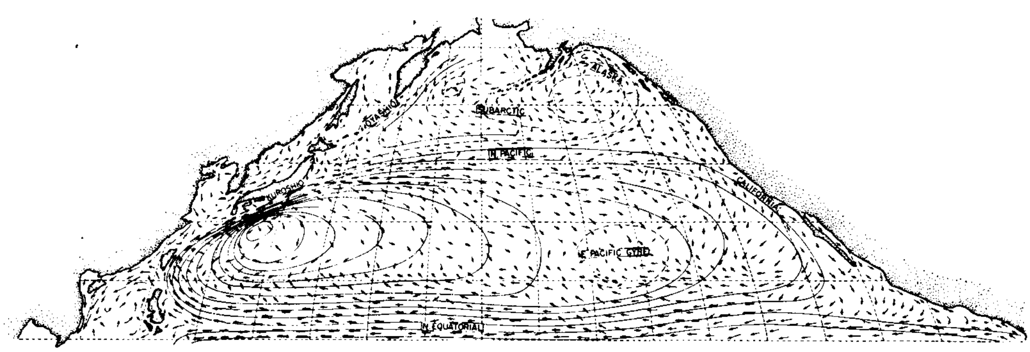

Fig. 7. Transport chart of the North Pacific as derived from oceanographic observations. Transport between adjacent stream lines are six million metric tons sec^{-1}. The stream lines are based on Fig. 205 of Sverdrup et al (1942), the arrows on the "Weltkarte zur Übersicht der Meereströmungen", Tafel 22, Deutsche Seewarte, *Ann. d. Hydrogr. u. Mar. Meteor.*, 1943. The projection is the same as the one in Figure 3.

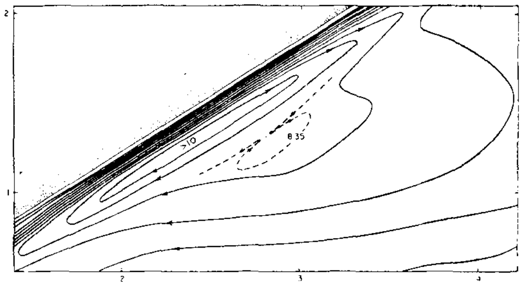

Fig. 8. Computed Pacific "Sargasso Sea" circulation in the triangular ocean basin for $A = 2.5 \cdot 10^7$ cm² sec⁻¹. This figure is an enlargement of the south-west portion of figure 4.

boundary by replacing boundary condition (4 b) with $\partial^2\psi/\partial\nu^2 = 0$ at $\xi = 0$, yields $b \approx + r'/\sqrt{3}$ (instead of $b \approx - r'/\sqrt{3}$), and

$$\psi'_{\max} = 1.30\, r' \sin \zeta \quad \text{at} \quad p\xi = 4\pi/3\sqrt{3}$$

instead of

$$\psi'_{\max} = 1.17\, r' \sin \zeta \quad \text{at} \quad p\xi = 2\pi/\sqrt{3}.$$

Thus with maximum velocity occurring directly against the boundary the western current has two-thirds its former width, and the transport is 20 per cent higher.

A more important modification may be related to the effect of the earth's rotation on lateral stress. Following the customary procedure we have, from analogy with the Navier-Stokes equations, introduced lateral stress into the integrated equations of motion through the term $A\nabla^2\mathbf{M}$. (WOC) Since the Navier-Stokes equations were derived for a resting coordinate system it would seem appropriate to replace the *relative* mass transport M by the absolute value $M + \mathbf{i}\,\Omega R h \cos\varphi$, where $\mathbf{i}$ is the unit vector pointing eastward, and h the effective depth of the current. Performing the curl operation[1] one obtains an additional term

$$A \frac{\partial^3}{\partial y^3}(\Omega R h \cos\varphi) = \frac{A\Omega h}{R^2} \sin\varphi$$

to be added to the wind curl on the right side of equation (1). Setting $A = 2.5 \cdot 10^7$ cm² sec⁻¹, $\varphi = 30°$, $h = 10^5$ cm, gives $2 \cdot 10^{-9} g$ sec⁻² compared to a wind curl of about $9 \cdot 10^{-9} g$ sec⁻². The effect would be to strengthen the transport in the subtropical gyre by about 25 per cent, to weaken the transport in the subpolar gyre, and to displace the boundary between the gyres northward.

The physical basis of this modification forms the substance of ROSSBY's (1936) discussion concerning the merits of Taylor's vorticity-transport theory and Prandtl's momentum-transport theory. If angular momentum is to be conserved, then any meridional interchange of eddies must induce a relative current setting eastward at high latitudes, and westward at low latitudes.

The discrepancy may also be ascribed to an underestimate of the surface stress for a given wind speed, especially at wind speeds of Beaufort four or less (WOC).

These remarks apply particularly to the western currents. In the case of the north equatorial current (of which only half is shown on figs. 4—6), the equatorial countercurrent, and the south equatorial current, SVERDRUP (1947) and REID (1948) have obtained satisfactory agreement between the transport computed from the wind stress and that computed from oceanographic observations.

[1] Here again we employ a plane coordinate system. In spherical coordinates the modification is several times larger. We hope to return to this problem in greater detail when considering a basin on a spherical earth.

The western boundary vortices (Sargasso Sea) and the value of A

An interesting feature is the double vortex system near the western boundary on figs. 4 and 5, which is shown on an enlarged scale on fig. 8. In the case of fig. 6 the small eastern vortex is absent, but its effect can still be noticed by the bulging of the stream lines.

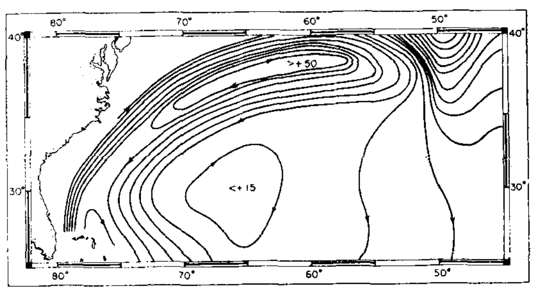

Fig. 9. Idealized topography of the sea level of the North Atlantic Ocean according to DEFANT (1941). The units are dynamic centimeters.

Whether the eastern vortex will or will not be present depends only on the width of the ocean and the value of the eddy viscosity, as will be seen from an inspection of equation (18). The curve in Fig. 2 represents a graph of the function $f(p\xi)$ in the bracket of equation (18) for an infinitely wide ocean ($\varepsilon = 0$). The function oscillates about the value of 1, and, strictly speaking, the vortex system extends to infinity, though the amplitudes of the vortices die off exponentially with distance from the western boundary. In the case of an ocean of (non-dimensional) width r' the function oscillates not about the horizontal line $f(p\,\xi) = 1$, but about the line $f(p\xi) = 1 - \varepsilon p\xi$. The eastern vortex exists only if the slope of the first term in the bracket of equation (18) at the distance $(p\xi)_m = 14\pi/\sqrt{3} = 8.45$, where it reaches its third maximum, exceeds the slope $-\varepsilon$ of the asymptotic line; that is, if

$$\varepsilon < \frac{2}{\sqrt{3}}\, e^{-\frac{1}{2}(p\xi)_m} \sin\left[\frac{\sqrt{3}}{2}\,(p\xi)_m\right] = 0.015.$$

The corresponding conditions on γ and A are:

$$\gamma < 0.015\, pr', \quad A < \frac{(0.015\, pr')^3\, \beta}{n^3}.$$

For the Pacific at latitude 30° N, $p = .445$, $r' = 8.6$, $\beta = 2 \cdot 10^{-13}$ cm^{-1} sec^{-1}, $\pi/n = 3\,900$ km, which gives $A < 8.25 \cdot 10^7$ cm^2 sec^{-1}. For the Atlantic at the same latitude, $\Theta \approx 50°$, $p = .625$, $r' = 6.0$, and $A < 7.8 \cdot 10^7$ cm^{2}sec^{-1} in order for the eastern vortex to exist.

In terms of the dynamic topography of the sea surface the double vortex system represents two humps in the sea surface, the western hump being much larger than the eastern hump (fig. 8). The two humps are separated by a trough running parallel to the western current with a saddle point directly between the humps. Observations in the Pacific Ocean are inconclusive with respect to the existence of the eastern hump. The corresponding area in the Atlantic, the Sargasso Sea, is one of the most intensely studied areas in the world, but even so the conclusions are uncertain. DEFANT's (1941) analysis of the dynamic topography based on observations from the *Meteor* expedition, and previous expeditions, is reproduced in fig. 9. It shows a small hump in the Bermuda area, but according to Defant (personal communication) the data was not quite convincing in this respect. At Defant's suggestion FELBER (1934) had previously analyzed the extensive observational material based on surface drifts of vessels, and his stream lines show a saddle point southwest of Bermuda throughout the year. His figure for April is reproduced in fig. 10.

Defant's and Felber's analyses are consistent with respect to the existence of a saddle point at about 70° west, 30° north, but they differ regarding the Gulf Stream countercurrent. This discrepancy has to do with the different methods of averaging employed by the two authors. The large number of observations[1] collected since Defant summarized the data in 1941 have made increasingly clear the variability of the circulation in the Bermuda area,

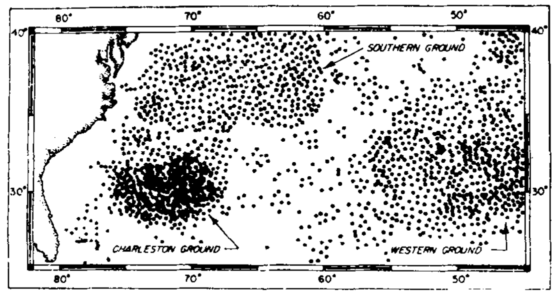

Fig. 11. Distribution of the sperm whale based on log-book records dating from 1761—1920 (according to TOWNSEND 1935). Each point represents the position of a whale ship on a day when one or more whales were taken.

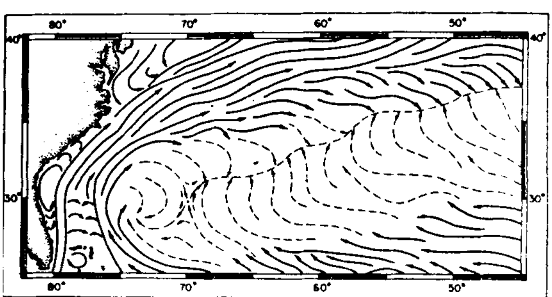

Fig. 10. Stream lines in the north-west Atlantic from the surface drift of ships, according to Felber (1934).

[1] We are indebted to C. O'D. Iselin, F. Fuglister, and A. Worthington of the Woods Hole Oceanographic Institut e for having made these observations available to us.

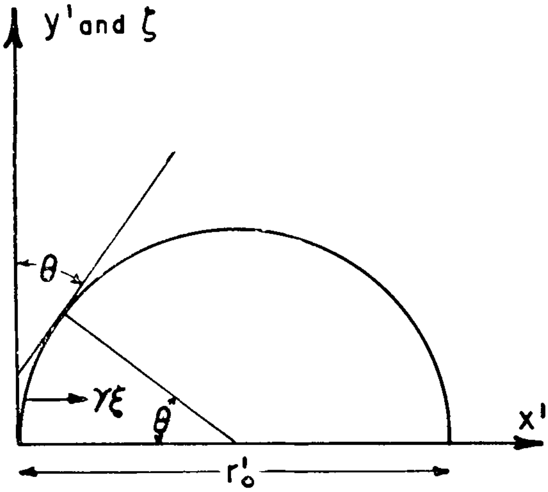

Fig. 12. Dimensions of semi-circular ocean basin.

and the shifting in position from season to season, even from week to week, of the Gulf Stream and related features (ISELIN and FUGLISTER, 1948). Defant's analysis is based on synoptic profiles, each of which reveals a countercurrent seaward of the Gulf Stream, occurring however at different locations for different cruises. Felber's averaging at fixed geographic location would naturally tend to obscure secondary features adjacent to strong but wandering primary features. The differences are somewhat similar to the differences between synoptic weather maps and climatic charts.

No suitable methods have yet been developed for combining results from different cruises to bring out the existence of secondary features such as the countercurrent and the eastern vortex. For this reason observations collected since 1941 have not added materially to our understanding of the Sargasso Sea circulation, but most of these observations indicate a north-flowing current west of Bermuda. A curious clustering in the distribution of sperm whales may perhaps be interpreted as evidence for the existence of the two vortices and the trough. Each point in fig. 11 represents the position of a whale ship on a day when one or more whales were taken, according to logbook records dating from 1761 to 1920 (TOWNSEND, 1935). Relatively few points are found in the region of the trough, yet there appear to have been no reasons for whaling ships to avoid this region. These troughs, according to Felber's presentation, are regions of convergence. In such regions the concentration of nutrients is small, and one may expect a relatively small concentration of plankton, and of sperm whales which feed on plankton. It is not impossible that the two vortices represent optimum conditions for the existence of plankton, these being the areas where freely floating organisms would remain for the longest time under uniform environmental conditions.

In a comparison of figs. 5—8 one must keep in mind that fig. 8 applies to the Pacific Ocean, whereas figs. 5—7 apply to the Atlantic. As a whole, the evidence, though far from conclusive, seems to support the existence of the eastern vortex, and would therefore indicate that the lateral eddy viscosity in this region is less than $7.8 \cdot 10^7$ cm^2 sec^{-1}.

The effect of curvature in the boundaries

It has been stated previously that the present method can be extended to an ocean basin of arbitrary shape provided the boundaries are not too irregular. To express this in quantitative form, consider a semi-circular basin of diameter (not radius) r'_0 (fig. 12). For a coordinate system we choose

$$\xi = \frac{x'}{\gamma} - \frac{r'_0}{2\gamma}(1 - \cos\Theta), \quad \zeta = \frac{r'_0}{2}\sin\Theta,$$

where, as previously, $\gamma\xi$ is the non-dimensional distance from the western boundary, Θ its inclination relative to a north-south direction, and r'_0 is the width of the basin at $y' = 0$. Differentiation leads to the same transformation as given by (10) except that Θ now depends on ζ. Neglecting variations in γ, we obtain

$$\nabla^2 = \frac{1}{\gamma^3}\left(\sec^2\Theta\frac{\partial^2}{\partial\xi^2} - \frac{2\gamma}{r'_0}\sec^3\Theta\frac{\partial^2}{\partial\xi\partial\zeta} + \ldots\right)$$

The second term is a correction for the curvature of the coastline. This correction is small provided the radius of curvature

$$\frac{1}{2}r'_0 \gg \gamma\sec\Theta.$$

As an extreme example of irregular boundaries consider the sharp change in the orientation of the eastern seaboard between Jacksonville, Florida, and Savannah, Georgia. Setting $\Theta = 0.04$ would require the radius of curvature to be large compared to .04 units of distance, or 40 km. The actual radius of curvature is 160 km.

Conclusions

The present method appears to be suitable for a numerical computation of the gross features in the ocean circulation, taking into account the outlines of the actual boundaries. The simple models discussed here give an indication of the results of such a computation. Changes in the orientation of the coast line will lead to a widening or narrowing of the western current, but the general features should be more or less the same, irrespective of the boundaries. This is in agreement with the fact that the general circulation is similar in the various oceans, whereas the ocean boundaries are not.

Acknowledgement

We are indebted to Mr P. Osborn for his assistance in preparing the figures.

REFERENCES

DEFANT, A., 1941: Die absolute Topographie des physikalischen Meeresniveaus und der Druckflächen, sowie die Wasserbewegungen im Atlantischen Ozean. *Deutsche Atlantische Exped. Meteor 1925—1927, Wiss. Erg.*, Bd **6**, 2 Teil, 5 Lief., fig. 41.

FELBER, O.-H., 1934: Oberflächenströmungen des Nordatlantischen Ozeans zwischen 15° and 50° n. B. *Arch. d. Deutschen Seewarte*, **53**, 1, pp. 5—17.

HIDAKA, K., 1949: Mass transport in ocean currents and the Lateral Mixing. *Geoph. Notes*, Tokyo Univ., **2**, 3, pp. 1—4.

ISELIN, C. O'D., and FUGLISTER, F. C., 1948: Some Recent Developments in the study of the Gulf Stream. *Journ. of Marine Res.*, **7**, (Sverdrup Anniv. Vol.) pp. 317—329.

MUNK, W. H., 1950: On the Wind-driven Ocean Circulation. *Journ. of Met.*, **7**, pp. 79—93.

REID, R. O., 1948: The Equatorial Currents of the Eastern Pacific as Maintained by the Stress of the Wind. *Journ. of Marine Res.*, **7**, pp. 74—99.

ROSSBY, C.-G., 1936: Dynamics of Steady Ocean Currents in the Light of Experimental Fluid Mechanics. *Pap. Phys. Oceanogr. and Met.*, **5**, 1, 43 pp.

SVERDRUP, H. U. and collaborators, 1942: The Oceans, Their Physics, Chemistry, and General Biology. Prentice-Hall, New York, 1087 pp.

SVERDRUP, H. U., 1947: Wind-driven currents in a baroclinic ocean; with Application to the Equatorial Currents of the Eastern Pacific. *Proc. Nat. Acad. Sci.*, **33**, pp. 318—326.

TOWNSEND, C. H., 1935: The Distribution of Certain Whales as Shown by Logbook Records of American Whale Ships. *Zoologic*, **19**, 1, pp. 2—50.